Defence Science Journal, Vol. 73, No. 5, September 2023, pp. 519-530, DOI : 10.14429/dsj.73.5.18315

Gait Parameter Tuning Using Bayesian Optimisation for an Alligator-Inspired Amphibious Robot

Atul Thakur

Department of Mechanical Engineering, Indian Institute of Technology, Patna - 801 106, India
E-mail: athakur@iitp.ac.in

ABSTRACT

This paper reports a sample-efficient Bayesian optimization approach for tuning the locomotion parameters of an in-house developed twelve degrees of freedom alligator-inspired amphibious robot. An optimization framework is used wherein the objective is to maximize the mean robot speed obtained via physical experiments performed on terrains with varying friction and inclinations and in the aquatic environment for swimming locomotion. We obtained an improvement in the mean robot speed by a factor of up to 6.38 using the developed approach over randomly generated locomotion parameters in 15 iterations.

Keywords: Bayesian optmisation; Bio-inspired robotics; Amphibious robotics

NOMENCLATURE

A_B : Amplitude for head, torso, tail joints (1 and 2)
A_H : Amplitude for hip joint
A_K : Amplitude for knee joint
$\Delta\varphi$: Phase lag between body joint actuators
E : Error angle between the robot orientation vector and goal
γ_B : Body offset parameter
γ_L : Leg offset parameter
H : Objective function
K_A : Acquisition function
K_D : Stochastic behavior of the objective function
K_E : Maximum objective evaluation
K_S : Number of seed points in the cost function
N : Number of active joints in the body
P : Gait parameter of robot $p \in \mathbb{R}^3 \mid p = [A_H \; A_B \; T]^T$
φ : The angle between goal and robot centroid
R : Radius of acceptance
S : The average speed of the robot in cm/s
T : The time-period in the gait cycle
T_{tr} : Time to travel from start to goal location
θ : Control action $\theta \in \mathbb{R}^{12} \left| \theta = \left[\theta_{B_i} \theta_{H_i} \theta_{K_i} \right]^T, i = 1,2,3,4. \right.$
θ_{B_i} : Commanded angle for i[th] body joint actuator, i = 1 to 4.
θ_{H_i} : Commanded angle for the i[th] hip joint actuator, i = 1 to 4.
θ_{K_i} : Commanded angle for i[th] knee joint actuator, i = 1 to 4.
$\bar{\theta}$: Robot orientation vector
x : State space vector $x \in \mathbb{R}^4 \mid \; x = \left[x_{c,1}, x_{c,2}, \dot{x}_{c,1}, \dot{x}_{c,2} \right]^T$
x_a : Position coordinated of red color marker $\left(x_a \in \mathbb{R}^2 \right)$
x_b : Position coordinated of green color marker $\left(x_b \in \mathbb{R}^2 \right)$
x_c : The centroid of the robot $\left(x_c \in \mathbb{R}^2 \right)$
x_g : Goal point $x_g \in \mathbb{R}^2$
x_o : Start point $x_o \in \mathbb{R}^2$

Received : 11 July 2022, Revised : 19 May 2023
Accepted : 24 May 2023, Online published : 31 August 2023

1. INTRODUCTION

Amphibious robotics has immense potential in various civil and defense applications such as resource exploration, disaster management, and reconnaissance. As a result, it has been attracting researchers' attention in recent years[1–4]. Among the different types of amphibious robots, those inspired by limbed amphibians have emerged as a promising avenue for research due to their relatively higher efficiency in terrestrial locomotion than their limbless counterparts. They can also swim by utilizing body undulation, making them an attractive source of inspiration for amphibious robot design[5]. Terrestrial locomotion in limbed amphibians is achieved by combining body undulation and leg oscillation-based gaits such as trot and creep. This results in an improved balance in the sagittal plane and higher energy efficiency[6-7].

Moreover, these creatures can tune their body undulations to a larger amplitude for terrestrial locomotion to enhance stability while the smaller amplitude and higher frequency for faster and energy-efficient swimming. However, tuning the locomotion parameters, including the frequencies and amplitudes of leg oscillations and body undulations, remains a critical challenge for designing amphibious robots inspired by limbed amphibians. The challenge encountered in tuning locomotion parameters is often due to the need for expensive physical experiments and the presence of sensor noise, which

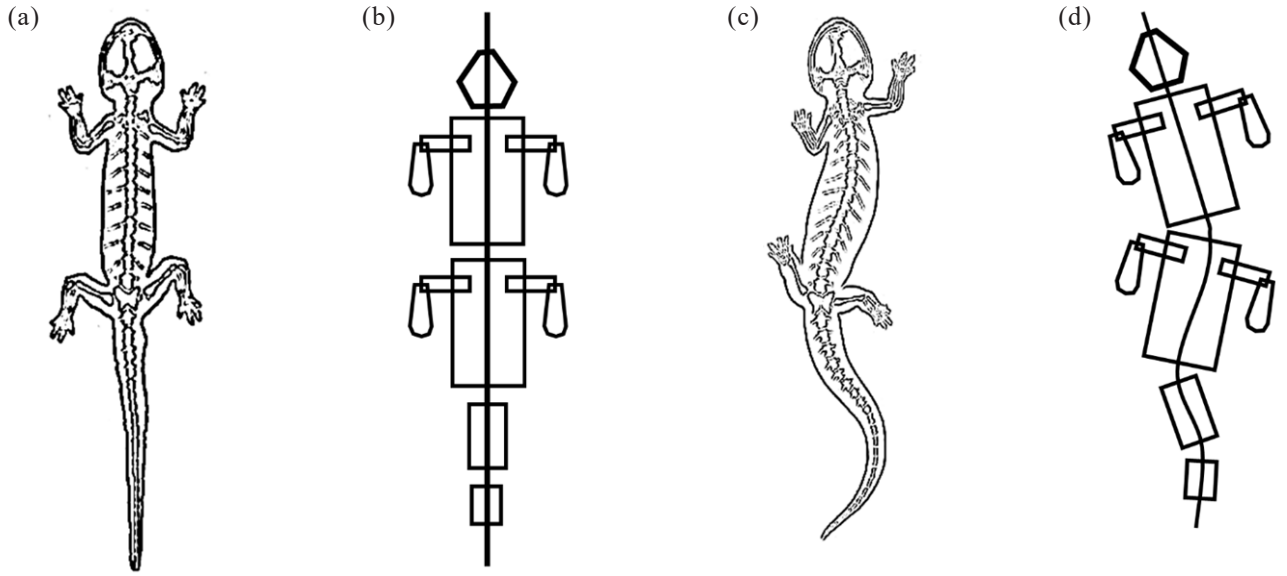

Figure 1. (a) Schematic of an alligator moving without undulations, (b) Alli-bot mimicking the motion without undulations, (c) Schematic of an alligator moving with undulations, and (d) Alli-bot mimicking the undulatory motions.

increases the complexity of the problem[8-9]. This paper presents a Bayesian optimisation-based, near globally optimal, noise-tolerant, and sample-efficient approach for tuning the gait parameters of both leg oscillation and body undulation to maximize the average speed of an in-house developed alligator-inspired amphibious robot. The developed technique offers an effective solution to the problem of locomotion parameter tuning in amphibious robotics, making it a significant contribution to the field.

Figure 1 depicts an alligator performing terrestrial locomotion using a combination of leg oscillation, body undulation, and a corresponding robotic implementation. The robot's locomotion depends upon the choice of the combination of parameters like joint amplitudes, frequencies, phase lags, and offset. It is challenging to develop a high-fidelity dynamics model of the robot's locomotion that can effectively capture the influence of friction and terrain geometry. Thus, a purely simulation-based approach for locomotion parameter tuning yields results fraught with the reality gap[10]. The most reliable way to tune the locomotion parameters is via performing physical experimental trials. However, conducting many experimental trials, especially using non-optimal parameters, may lead to a rapid wear-and-tear of the robotic platform and is thus expensive and tedious. Also, the experimental fitness evaluation is plagued with noise and uncertainty due to the use of sensors.

In this paper, we aim to reduce the number of experimental trials needed for estimating locomotion parameters using Bayesian optimisation. It offers a gradient-free approach for global optimisation of functions with stochastic and expensive function evaluations[11]. Using Bayesian optimisation, we arrived at the optimal set of gait parameters by performing minimal experiments.

We first parameterised the robot gaits in terms of amplitudes and frequencies of leg oscillations and body undulations. After this, we developed an approximate robot simulation model, which we used for estimating the settings like acquisition function, stochastic behavior of the objective function, maximum number of objective evaluations, and Bayesian optimisation routine seed points. Finally, we employed Bayesian optimisation using the settings determined from the simulations to optimize the locomotion parameters from the physical experiments.

In the past, we reported applying Bayesian optimisation for the terrestrial locomotion parameter optimisation for an in-house developed quadruped alligator-inspired robot[12]. In this paper, we extend the earlier approach to include aquatic locomotion.

2. LITERATURE REVIEW

Examples of robots inspired by mammalian locomotion are cheetah-cub[13], BigDog[14], LittleDog[15], and MIT Cheetah 2[16]. On the other hand, examples of amphibious robots include Salamander robot[17], Amphi-Hex 1[2], flexible flipper leg-based robot[18], Alli-bot[19], and an alligator-inspired modular robot[20]. Both static and dynamic stability[21] and active and passive walking have been extensively researched[22] in the case of legged robots. Some legged robot designs, such as TITAN XII[23], ANYmal[24], and the SCOUT[25,] are not bio-inspired.

In locomotion control, Kurazume[26-27] developed a feedforward and feedback dynamic trot gait control system for Titan-VIII. Gehring et al. created dynamic gaits for a quadrupedal robot dealing with random perturbations to travel optimally at a certain speed[28]. Maleki et al. presented a control and gait design with an active spine for energy efficiency[29]. Horvat et al. developed a reflex-based controller for a salamander-like robot walking on an uneven terrain[30]. Liang et al. show a set of control algorithms based on SLIP (Spring Loaded Inverted Pendulum) to regulate the forward and lateral running speed, hopping height, and body attitude[31].

Alligator exhibits different types of gaits, of which trot is the high walking gait and is used for drier and hard terrains with a duty factor of 0.73 to 0.83 and a speed range of 0.16±0.01 m/s[32]. They have uncanny reptilian locomotion,

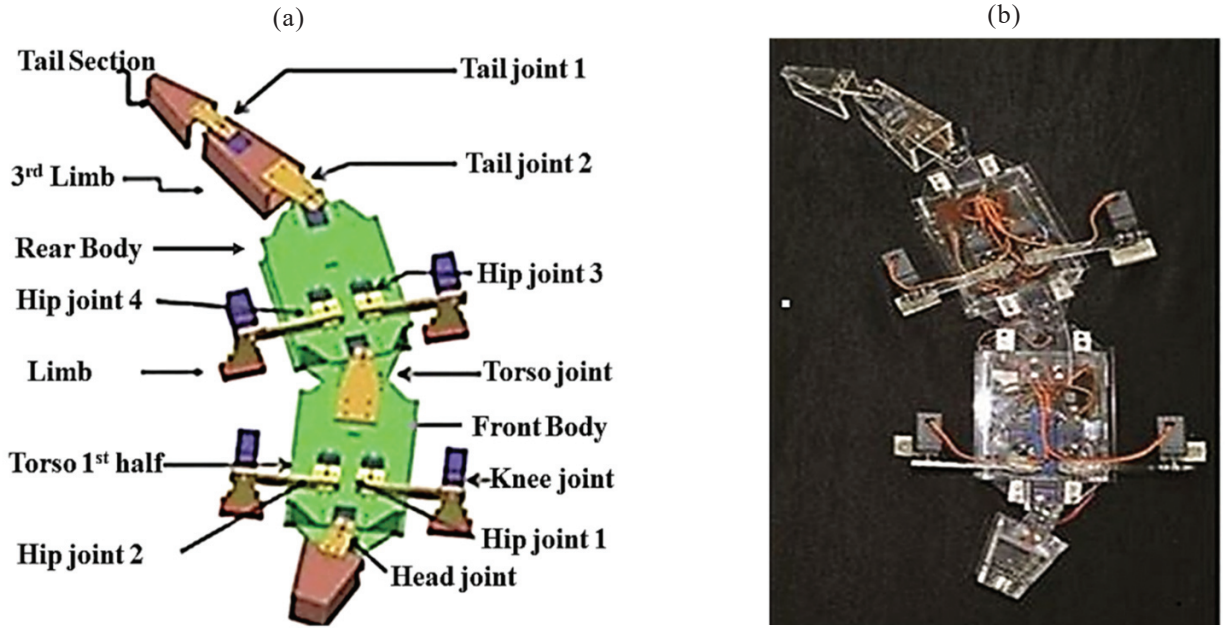

Figure 2. (a) 3D model of the robot, and (b) Fabricated prototype of the robot.

which is considered as a next step in the evolution of vertebrate locomotion[33–35]. Their tail accounts for nearly 28 % of body weight, so hind limbs support an increased percentage of weight when a quadruped is working against a drag[32]. Alligators employ sharp amplitude variations, identified as a major thrust generator, from head to tail with a mean amplitude varying between 0.07 and 0.10 times the body length[20]. Tails of the mammalians play an essential role in dynamic stability, maneuverability, and speed[32]. To the best of our knowledge, the roboticists have not investigated the effect of the tail on the speed of a legged bio-inspired robot.

In the case of aquatic locomotion, serpentine and Anguilliform gaits are mainly studied for limbless robots inspired by eel or lamprey and utilise active body undulation[36-37]. Swimming in robots with both active limbs and spine has been studied in Salamander Robotics II, wherein limbs are actively used for terrestrial locomotion while an active spine causing body undulation is used for aquatic locomotion[5].

In the area of gait optimisation, reinforcement learning has been applied by various researchers like Saggar et al.[38], Erden and Leblebiciouglu[39], and Li et al.[40]. Rofer used evolutionary algorithms to optimize the gait parameters for a quadruped in the Sony Four-Legged Robot League[41]. Chernova and Veloso used an evolutionary approach based on genetic algorithms to optimize the gait of the Aibo robot[42]. Weingarten et al. used the Nelder-Mead algorithm to optimize the gait speed for a hexapod[43]. Kohl and Stone compared different optimisation algorithms, namely hill climbing, Amoeba (Nelder-Mead algorithm), genetic algorithms and policy gradient reinforcement learning, to improve the forward speed of quadruped robots in an offline setting[44]. Santos et al. explored the idea of gait transitions in a quadruped robot based on the robot speed and behavioral context of the robot[45]. Koco et al. employed the Genetic Algorithm to optimize a multiobjective function to tune the foot trajectories parameters in open loop control for achieving optimal energy and fast robot locomotion[46].

Gehring et al. developed an optimisation-based approach to control the agile motion of a quadrupedal robot by automatically fine-tuning the controller parameters by repeatedly executing slight variations of the same motion task[47]. Digumarti, *et al.* developed an approach for optimizing the robot's morphology and tuning the control parameters for trotting and bounding gait simultaneously while achieving a certain speed[48]. RunBin et al. reported a time-pose control method for a trotting gait on two terrains: flat and inclined in real-time[49].

Calandra et al. applied Bayesian optimisation for learning biped gaits and compared the same with other optimisation techniques[11].

We have combined the online and offline procedures described in Fig. 2 for Alli-bot. At first, we run the Bayesian optimisation algorithm over numerical simulation to tune the algorithm's hyperparameters (K_A, K_D, and K_S) and to determine the minimum number of iterations required (K_E). Next, we run the Bayesian optimisation algorithm over the physical robot using the tuned hyperparameter values to get the optimal gait parameters (A_k, $A_{b,}$ and T).

The main contributions of this paper include: (1) the development of a parameterized simulation model for Alli-Bot, (2) a Bayesian optimisation approach to determine optimal gait parameters for Alli-Bot on the simulator, (3) a physical experimental platform for validating the determined optimal parameters on different terrains.

3. DESIGN, FABRICATION, AND SIMULATION OF THE ALLIGATOR-INSPIRED PLATFORM

Alli-bot is an alligator-inspired robot having 12 degrees of freedom (DOF). It combines limb oscillations and body undulations for terrestrial locomotion, while the body undulations alone for aquatic locomotion (see Fig. 2). Each of its limbs has two revolute joints, namely hip, and knee, and four revolute joints, namely neck, torso, tail 1, and tail 2 on the body. The hip joint is proximal, while the knee joint is distal

on each leg of the Alli-bot. While walking, the entire body of the Alli-bot is supported by its limbs. The body of the robot is divided into 5 parts connected by four servo motors; head joint connects the head and torso's 1st half, the torso joint connects the two halves of the torso and the tail joint 2 connects the third link with the posterior half of the torso and lastly the tail joint 1 which connects the two tail sections. We fabricated all the links using laser cutting, and more details of the same can be found in[47]. We used 12 HK 15328D servomotors with a maximum torque capacity of 12 kg-cm for actuating the robot joints.

We developed a simulation model of our Alli-bot in CoppeliaSim (formerly known as V-REP)[50] (see Fig. 3). Firstly, the CAD model of Alli-bot was imported in CoppeliaSim, and then the geometry was extracted using cuboidal meshes. Now we matched the weight, maximum torque, and speed of each servomotor in the simulator environment with those of real values. In the simulation, we kept the friction coefficient between the ground and robot contact point 1.0 to provide maximum force in the forward direction during locomotion. Collision detection was enabled to detect and thereby avoid self-collisions. To avoid self-collision, we also kept the maximum amplitude range for the knee and body to be 35 and 40 degrees. OpenDynamics engine was used in CoppeliaSim[50] for the dynamics of the developed model.

Two types of forces due to the surrounding water were modeled for underwater simulation. Firstly, the buoyancy due to each link was determined using $F_{buoyancy}=\rho_f V_f g$, where ρ_f is the density of water, V_f is the volume of water, and g the acceleration due to gravity. Secondly, the drag due to the robot movement in water was determined using $F_{drag} = F_l + F_A$, where, $F_l = c_l v_{link}$ is the linear drag and F_A is the added mass, with c_l being the drag coefficient matrices. The values of the coefficients were manually tuned to match the simulation approximately to the behaviour of the physical robot. As the objective of this paper is to finally tune the locomotion of the physical robot using Bayesian optimisation, more sophisticated approach to perform system identification was not pursued and would be explored in future work.

4. GAIT DESIGN

Parameterized cycloidal trot gait functions are developed with amplitude and time- period as parameters, to emulate the alligator's motion on the robot. A cycloidal function is used to obtain a smooth movement of the robot along with body undulation. The cycloidal joint functions designed for the robot are presented as follows:

The hip and body joint motions are governed by Eqn. (1) – Eqn. (3):

$$\theta_{H_{1,2}} = \begin{cases} 2A_H\alpha_1 - A_H + \gamma_L & 0 \le t < \frac{T}{6} \\ A_H + \gamma_L & \frac{T}{6} \le t < \frac{T}{2} \\ 2A_H(1-\beta_1) - A_H + \gamma_L & \frac{T}{2} \le t < \frac{2T}{3} \\ -A_H + \gamma_L & \frac{2T}{3} \le t < T \end{cases} \quad (1)$$

$$\theta_{H_{3,4}} = \begin{cases} 2A_H(1-\alpha_1) - A_H + \gamma_L & 0 \le t < \frac{T}{6} \\ -A_H + \gamma_L & \frac{T}{6} \le t < \frac{T}{2} \\ 2A_H\beta_1 - A_H + \gamma_L & \frac{T}{2} \le t < \frac{2T}{3} \\ A_H + \gamma_L & \frac{2T}{3} \le t < T \end{cases} \quad (2)$$

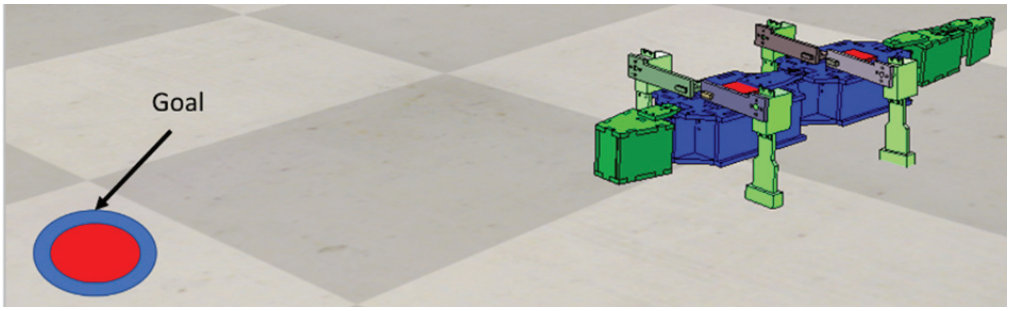

Figure 3. Simulation model of Alli-bot developed in CoppeliaSim[50].

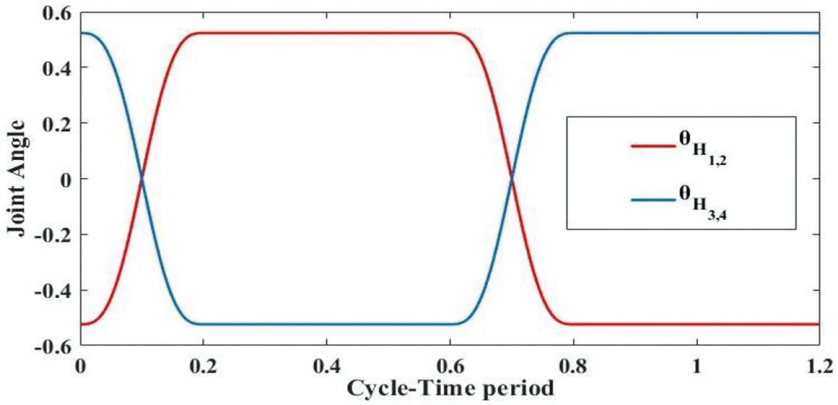

Figure 4. Variation of hip-joint angle with time.

$$\theta_{B_i} = A_B \sin(2\pi \frac{t}{T} + 2\pi\Delta\varphi(i-1)) + \gamma_B \quad (3)$$

where, $\alpha_1 = \frac{6t}{T} - \frac{\pi}{2}\sin(\frac{12\pi t}{T})$ and $\beta_1 = \frac{6(t-\frac{T}{2})}{T} - \frac{\pi}{2}\sin(\frac{12\pi t}{T})$ and t is the running time of the current experiment, T is the joint oscillation period, A_H is the hip amplitude, and γ_L is the offset.

The knee joint motions are governed by Eqn. (4) - (7):

$$\theta_{K_1} = \begin{cases} 0 & 0 \le t < \frac{T}{4} \\ -A_K\alpha_2 & \frac{T}{4} \le t < \frac{5T}{12} \\ A_K & \frac{5T}{12} \le t < \frac{3T}{4} \\ A_K(1-\beta_2) & \frac{3T}{4} \le t < \frac{11T}{12} \\ 0 & \frac{11T}{12} \le t < T \end{cases} \quad (4)$$

$$\theta_{K_2} = \begin{cases} -A_K & 0 \le t < \frac{T}{4} \\ -A_K(1-\alpha_2) & \frac{T}{4} \le t < \frac{5T}{12} \\ 0 & \frac{5T}{12} \le t < \frac{3T}{4} \\ -A_K\beta_2 & \frac{3T}{4} \le t < \frac{11T}{12} \\ -A_K & \frac{11T}{12} \le t < T \end{cases} \quad (5)$$

$$\theta_{K_3} = \begin{cases} A_K & 0 \le t < \frac{T}{4} \\ A_K(1-\alpha_2) & \frac{T}{4} \le t < \frac{5T}{12} \\ 0 & \frac{5T}{12} \le t < \frac{3T}{4} \\ A_K\beta_2 & \frac{3T}{4} \le t < \frac{11T}{12} \\ A_K & \frac{11T}{12} \le t < T \end{cases} \quad (6)$$

$$\theta_{K_4} = \begin{cases} 0 & 0 \le t < \frac{T}{4} \\ -A_K\alpha_2 & \frac{T}{4} \le t < \frac{5T}{12} \\ -A_K & \frac{5T}{12} \le t < \frac{3T}{4} \\ -A_K(1-\beta_2) & \frac{3T}{4} \le t < \frac{11T}{12} \\ 0 & \frac{11T}{12} \le t < T \end{cases} \quad (7)$$

where, $\alpha_2 = \frac{6(t-\frac{T}{2})}{T} - \frac{\pi}{2}\sin(\frac{12\pi(t-\frac{T}{4})}{T})$ and $\beta_2 = \frac{6(t-\frac{3T}{4})}{T} - \frac{\pi}{2}\sin(\frac{12\pi(t-\frac{T}{4})}{T})$ and A_K is the knee amplitude, and $N\Delta\varphi$ is the total phase lag between head and tail. N is the number of active joints in the robot's body, which is 4 in our case. An undulation with $N\Delta\varphi$=1.0 corresponds to an undulation in which the body makes a complete wave (see Fig. 4 and Fig. 5).

5. EXPERIMENTAL SETUP

A line-of-sight (LOS) guidance law is employed in the experimental setup, where the error angle between the specified goal and robot is calculated using the overhead camera, which acquires the images of the color labels (see Fig. 6). LOS-based guidance helps in tracking the waypoints[51]. A grid-based calibration was performed to determine the distance represented by one pixel at different points in the camera's field-of-view to prevent perspective error in the overhead camera measurement.

The acquired images are processed to detect three color markers using a colour-based thresholding scheme; two of the labels are situated on the front body and the rear body to determine the orientation, and one is to detect the goal location. While orientation detection using the overhead camera and color markers is effective for terrestrial gait on a 2D surface, it presents several challenges for detecting 3D motion in aquatic environments. More advanced motion detection technologies such as SONAR can be utilized for underwater localization to overcome the challenges as mentioned earlier. However, it is

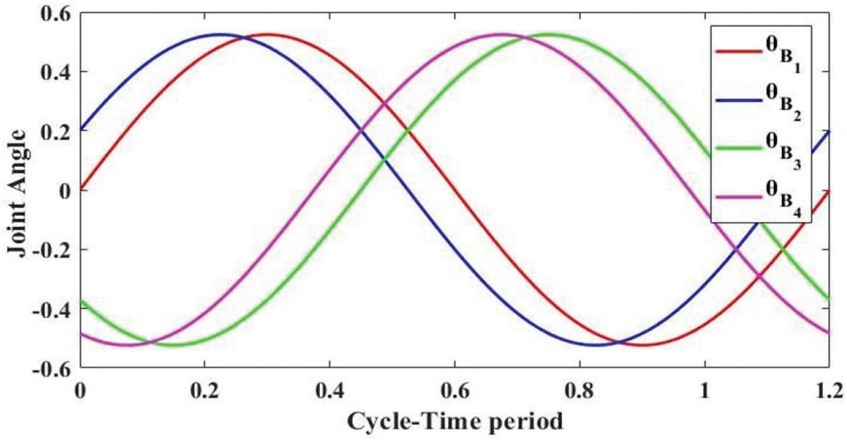

Figure 5. Variation of body joints angles with time.

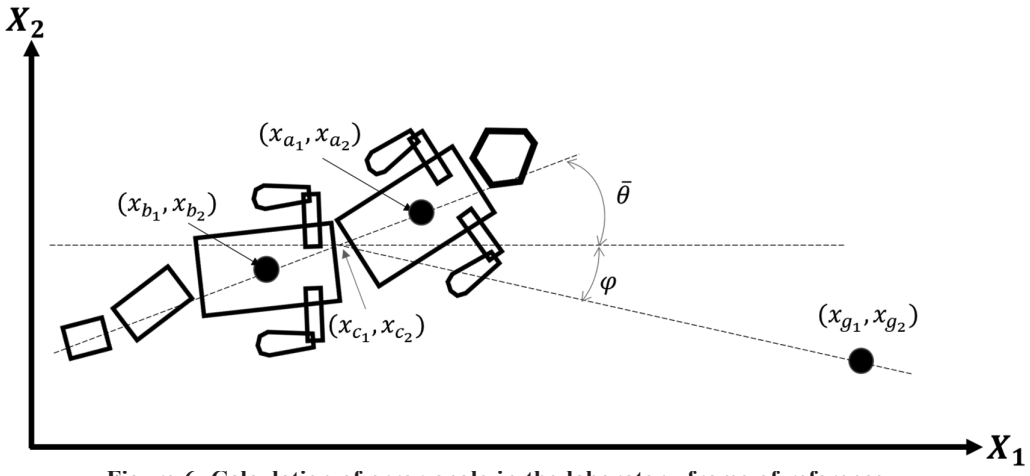

Figure 6. Calculation of error angle in the laboratory frame-of-reference.

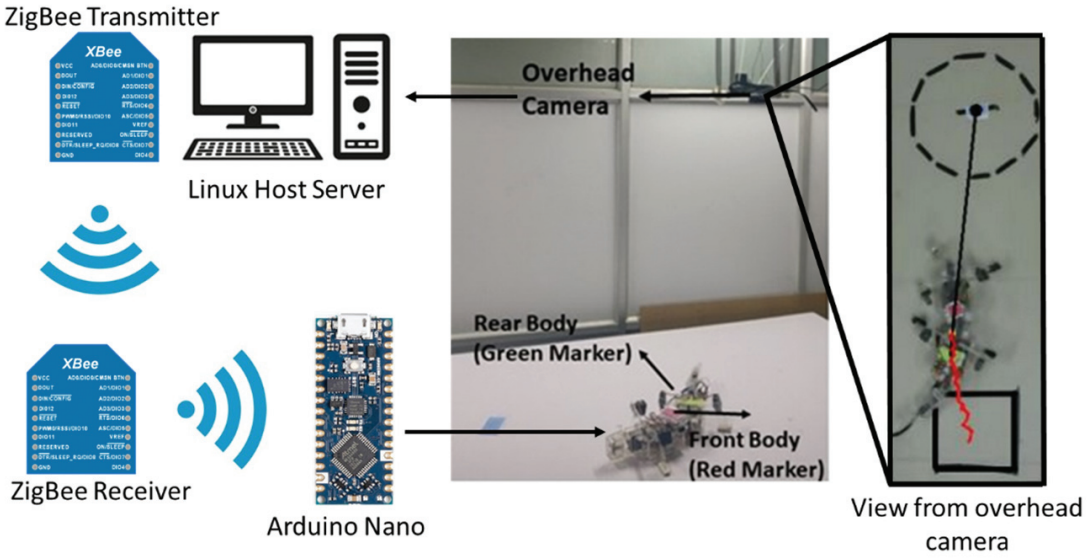

Figure 7. Experimental setup.

worth noting that the same overhead camera technique has been employed for underwater localisation with certain assumptions in place. Firstly, it has been assumed that the robot moves in a single plane while underwater. Additionally, it has been assumed that the robot remains close to the water surface to minimize any distortions caused by refraction. However, in the future, experiments with SONAR-based localization system may also be performed to capture 3D motions.

The host PC is used to calculate the error angle, and ZigBee is used to communicate the error angle to the robot. We implemented a PD controller for closed-loop control, and the computed error angle is used to calculate the offset parameters γ_B and γ_L for body and legs of the gait Eqn. (1), (2) and (3), respectively as follows:

$$\gamma_B = K_{P_B} e + K_{D_B} \dot{e} \tag{8}$$

$$\gamma_L = K_{P_L} e + K_{D_L} \dot{e} \tag{9}$$

$$e = \varphi - \bar{\theta} \tag{10}$$

where, $\bar{\theta}$ is the robot orientation vector, which is calculated by $\bar{\theta} = \tan^{-1}\left(\frac{x_{a,2} - x_{b,2}}{x_{a,1} - x_{b,1}}\right)$ and $\varphi = \tan^{-1}\left(\frac{x_{g,2} - x_{c,2}}{x_{g,1} - x_{c,1}}\right)$, $x_c = \begin{bmatrix} \frac{x_{a,1} + x_{b,1}}{2} & \frac{x_{a,2} + x_{b,2}}{2} \end{bmatrix}^T$ is the centroid of the robot, x_a and x_b are determined using the overhead camera, K_{P_B}, K_{D_B}, K_{P_L}, and K_{D_L} are controller gains that are tuned manually.

Computed offsets are then used in the gait function Equations (1), (2), and (3) to generate the command for the twelve servomotors. The above scheme (see Fig. 7) is used for commanding and moving the robot between a specified starting and goal location, separated by a distance of 1 m on the floor. We use a circle of acceptance of a radius 20 cm around the goal location. The ZigBee used has an indoor/urban range of up to 60 meters (200ft). The hand-tuned values of K_{P_B} and K_{P_L} vary between [0.8, 0.9] and K_{D_B} and K_{D_L} vary between [0.1 , 0.25] for the set of parameters used in the experiments reported in this paper.

6. GAIT PARAMETER TUNING USING BAYESIAN OPTIMISATION

With the parameterization described above, the problem of optimizing the gait speed becomes a parameter optimisation problem in multi-dimensional space. Various algorithms exist to solve the problem, but the selected approach must possess the following characteristics. The algorithm should satisfy several requirements. Firstly, it should be gradient-free since the dynamical parameters of the system are not entirely known. Additionally, it should have a fast convergence rate and be capable of finding the global optimum irrespective of the initial seed point. Finally, it should account for the stochastic nature of the objective function.

Physical experiments are expensive in terms of time and wear-tear of the robot. Also, the robot's motion often involves uncertainties due to the sensing noise. To optimize the locomotion parameters for maximizing the robot speed, we need a model that accounts for stochasticity and can be estimated from a minimum number of physical experiments. We used Gaussian Process Regression (GPR) to develop a surrogate model for the robot motion to meet the requirements above[52]. In BO, the GPR is initialized with random points from the parametric space, and then a new point is acquired and evaluated from the parametric space to improve the GPR. The process above is continued, and we arrive at a near-optimal point in the parametric space. We defined the objective function for optimisation as follows:

$$h(p; x_o, x_g): \mathbb{R}^3 \rightarrow \mathbb{R}^1 \tag{11}$$

where, h is the objective function which returns the maximum speed by the robot to go from the initial location x_o to a specified goal location x_g with p as the gait parameter. The following equation can specify the dynamics of the robot's motion:

$$\dot{x} = f(x,u) \tag{12}$$

where, f is the dynamical model of the robot, $x = [x_{c,1}\, x_{c,2}\, \dot{x}_{c,1}\, \dot{x}_{c,2}]^T$ is the state vector $[x_{c,1}\, x_{c,2}]^T$ is the coordinate and $[\dot{x}_{c,1}\, \dot{x}_{c,2}]^T$ is the velocity of the robot centroid expressed in the laboratory frame of reference. The term u represents the control functional defined as:

$$\theta = u(e; p) \tag{13}$$

where, the error angle e is determined using a line-of-sight guidance law $e = \varphi - \bar{\theta}$ which is explained in the previous section, $x_o = \begin{bmatrix} x_{o,1}\, x_{o,2} \end{bmatrix}^T$ and $x_g = \begin{bmatrix} x_{g,1}\, x_{g,2} \end{bmatrix}^T$ are the robot centroid's initial and goal locations, respectively. The parameter p is a 3-tuple $p = [A_H\, A_B\, T]^T$ and the control signal is defined as 12-tuple $\theta = \begin{bmatrix} \theta_{B_i}\, \theta_{H_i}\, \theta_{K_i} \end{bmatrix}^T$ where, θ_{H_i} are the hip joint angles, θ_{K_i} are the knee joint angles, and θ_{B_i} are the body joint angles.

The objective function is defined as $h = -\dfrac{\|x_o - x_g\|}{T_{tr}}$, T_{tr} is the traveling time required for the robot to go from x_o to x_g. The traveling time T_{tr} is computed by solving the following Eqn.:

$$\int_{x_0}^{x_g} dx = \int_{0}^{T_{tr}} f(x,u)dt \tag{14}$$

A closed-form solution for Eqn. 12 cannot be determined, and hence we have used experimental evaluation on physical and simulated platforms to evaluate T_{tr}. We can now define the optimisation problem as:

$$p^* = \arg\min_{p}\ h(p; x_o, x_g) \tag{15}$$

To solve the above problem we use Bayesian Optimisation $BO(h(p; x_o, x_g); K)$ where, K is the hyperparameter of the Bayesian optimisation function, namely *bayesopt* in the Statistics and Machine Learning toolbox of Matlab™. Here, the objective function works on minimizing negative speed, which is equivalent to maximizing speed. The hyperparameters of *bayesopt* include the acquisition function K_A, stochastic behavior of the objective function K_D, which appears in Matlab as 'Is Objective Deterministic', the maximum number of objective evaluations K_E, and K_S seed points. We have used the acquisition function expected-improvement plus (EI-plus).

Tesch, *et al.* show that EI converges faster than other acquisition functions[53]. The Matlab™ function *bayesopt* offers the facility for having a tradeoff between exploration and exploitation. *EI-plus* in *bayesopt* has the propensity to explore, and also it escapes a local objective function minimum by avoiding overexploiting an area. Also, we set the objective function as stochastic by selecting the option K_D as false to account for the actuation uncertainties and the sensor noise.

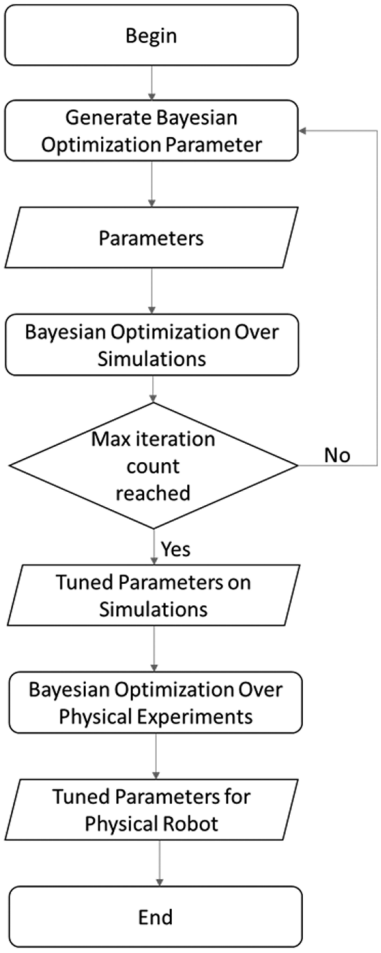

Figure 8. An overview of the approach used for locomotion parameter tuning of Alli-bot.

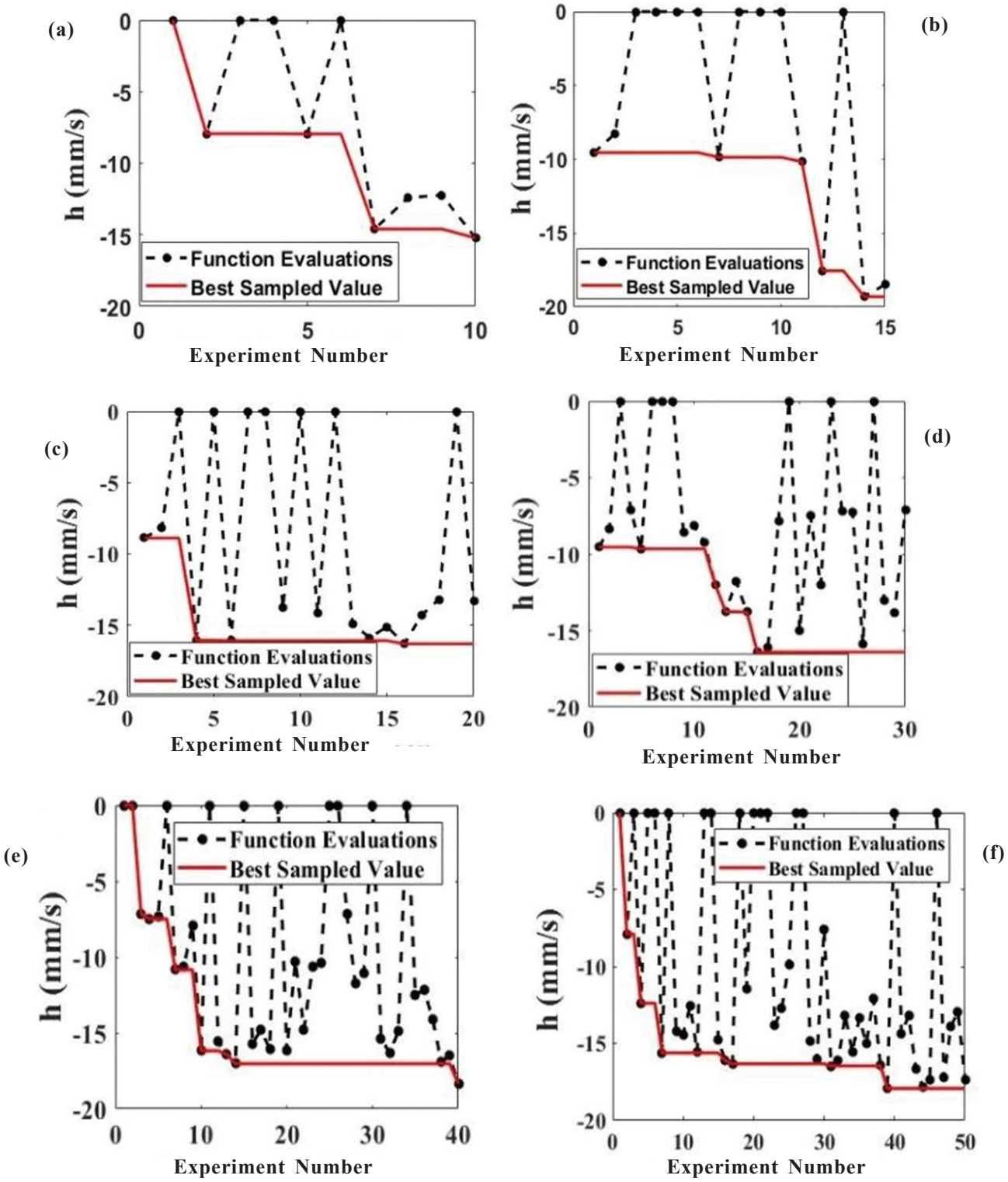

Figure 9. Optimisation of robot speed in simulation with (a) K_E=10 and K_S=3 (b) K_E==15 and K_S=3 (c) K_E==20 and K_S=3 (d) K_E==30 and K_S=3 (e) K_E==40 and K_S=4 (f) K_E==50 and K_S=5.

Further, an initial population is required to be able to make an initial model, so we selected the value of K_S as 3. An overview of the optimisation approach has been depicted in Fig. 8.

We performed simulations to determine the maximum number of objective evaluations K_E. To determine the suitable value of K_E, we performed a binary search. For that, we ran the BO over the simulations with K_E values 10, 20, 30, 40, and 50 (see Fig. 11 and Fig. 12). We found that K_E values of 10 and 20 yielded a significant reduction in the objective values compared to the other intervals. We then searched K_E using the same approach in the range 10 to 20. Based on the search mentioned above, we selected K_E *=15* for the experiments.

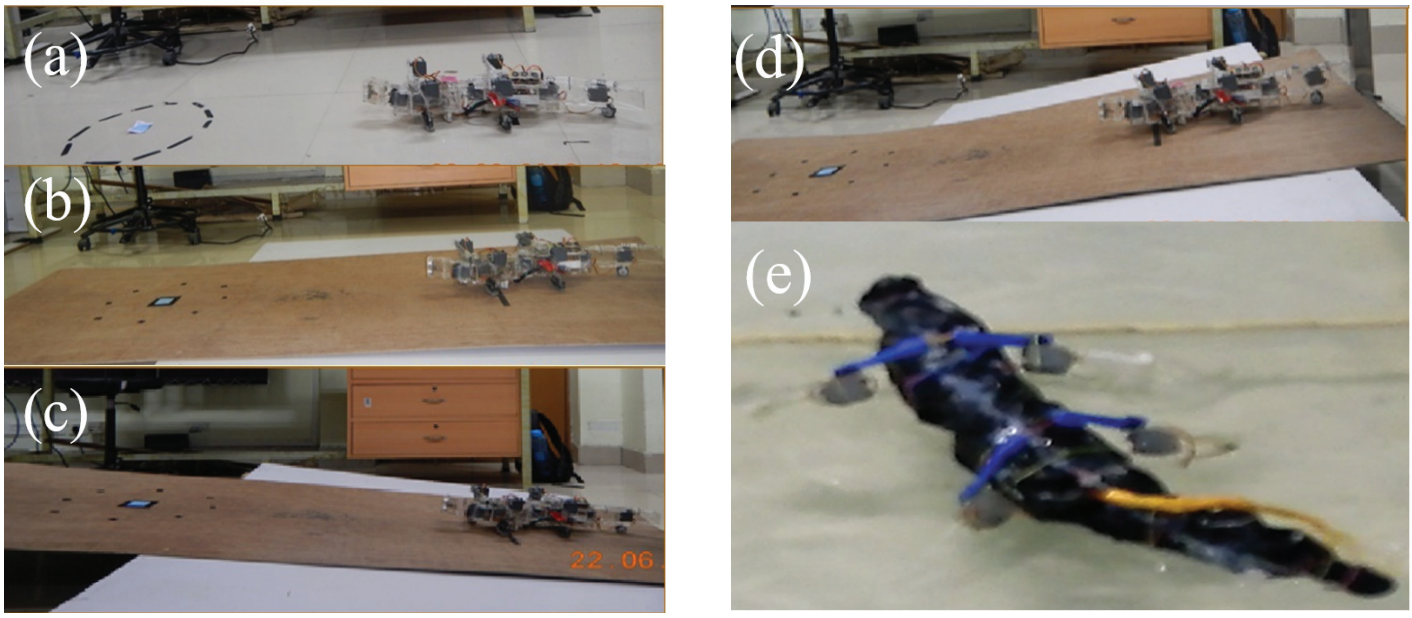

Figure 10. Details of terrains on which gait tuning was performed: a) flat terrain with low friction surface, b) flat terrain with high friction, c) rough terrain with 5° slope, d) rough terrain with -5° slope, and e) swimming in water.

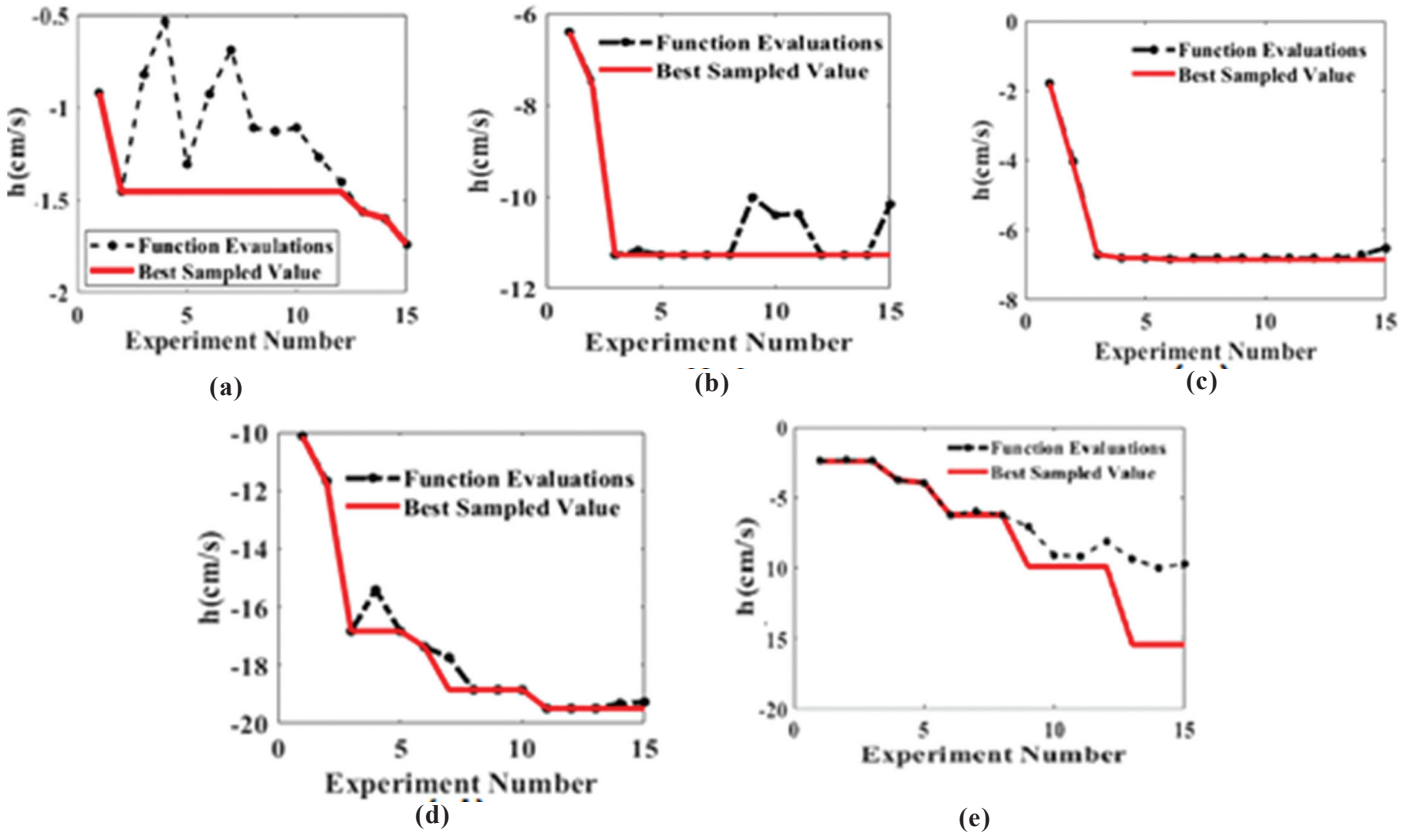

Figure 11. Optimisation results for K_E=15 and K_S=3 for physical experiments: (a) flat terrain with low friction surface, (b) flat terrain with high friction, (c) rough terrain with 5° slope, (d) rough terrain with -5° slope, and (e) swimming in water.

From the simulations, we observed that 30, 40, and 50 values for K_E tend to give nearly an improvement of 18 mm/s (see Fig. 9).

Using the hyperparameter values, thus determined K_A = *EI-Plus*, K_D = *false*, K_E =*15*, and K_S =*3*, we obtained optimized parameters from the simulation, which are A_K= 23°, A_B= 28°, and T=3.1*s*. Further, the hyperparameters determined previously from the simulations are used for running BO over the physical experiments. Using BO, the other parameter values are determined, and then the physical experiment was run to obtain the average speed. For each parameter value, we performed three experiments and determined the mean robot speed to capture the stochasticity caused due to sensor noise and actuator uncertainty. The average speed, thus determined, was

Table 1. Results of parameter tuning for different terrains

Terrain	Slope	Speed (cm/s) obtained from hand-tuned parameters	Speed (cm/s) obtained after tuning from Bayesian optimisation	Optimized gait parameters	Factor of improvement
Flat terrain with low friction	0˚	0.90	1.74	[A_K= 22°, A_B= 30°, T=5.6s]	1.93
Flat terrain with high friction	0˚	6.27	11.27	[A_K= 29°, A_B= 22°, T=3.06s]	1.79
Upward slope	+5˚	1.78	6.85	[A_K= 30°, A_B= 15°, T=3.07s]	3.85
Downward slope	-5˚	10.13	19.49	[A_K= 29°, A_B= 27°, T=3.55s]	1.85
Swimming in water	-	2.41	15.43	[A_B= 29°, T=3.92s]	6.38

used in BO as the objective function value, and then the other parameter values were computed. The process was repeated for 15 iterations for different terrain and also for swimming. We obtained the optimized parameters for flat terrain with a smooth surface [A_K= 22°, A_B= 30°, T=5.6s]. The corresponding robot average speed was found to be 1.74 cm/s.

The robot speed obtained for random parameter values was 0.9 cm/s. We thus found an improvement by a factor of 1.93. For flat terrain with a rough surface, the corresponding average speed was found to be 11.25 cm/sec. The robot speed obtained for random parameter values was 6.27 cm/s. We obtained the optimized parameters for flat terrain with rough surface [A_K= 29°, A_B= 22°, T=3.06s]. Speed improvement is about 76 % for +5° slope terrain by a factor of 3.85 i.e. from 1.786 cm/s to 6.85 cm/s. We obtained the optimized parameters [A_K= 30°, A_B= 15°, T=3.07s]. For – 5˚ slope terrain improvement is about in speed is about 1.85 times, i.e., 10.13 cm/s to 19.49 cm/s. We obtained the optimized parameters [A_K= 29°, A_B= 27°, T=3.55s]. For swimming improvement in speed is about 6.38 times i.e., from 2.415 cm/sec to 15.43 cm/sec.

We obtained the optimized parameters [A_B= 29°, T=3.92s]. Figure 10 shows the details of various terrains on which the physical experiments were performed and the gait parameters were tuned. Figure 11 depicts the optimisation results obtained from the physical experiments. The optimisation results obtained for various terrains are summarised in Table 1.

7. CONCLUSIONS

This paper reports the design, fabrication, and locomotion control of a 12-DOF alligator-inspired amphibious robot called Alli-bot. We developed a CoppeliaSim-based simulation model for Alli-bot. We also designed parameterized cycloidal gait for leg oscillation and body undulation for the smooth motion of the robot. The parameters of the designed gait pattern were determined using Bayesian optimisation. We determined the hyperparameters of Bayesian optimisation using simulations and then used the same for optimizing gait parameters from physical experiments. The improvement factor in the robot's speed has ranged from 1.79 for flat terrain with friction to 6.38 for swimming. In the future, we aim to incorporate specific energy consumption into the objective function and thereby optimize the same.

REFERENCES

1. Crespi, A.; Badertscher, A.; Guignard, A. & Ijspeert, A. J. AmphiBot I: an amphibious snake-like robot, *Robotics and Autonomous Syst.*, 2005, **50**(4), 163-175. doi: 10.1016/j.robot.2004.09.015..
2. Liang, X.; Xu, M.; Xu, L.; Liu, P.; Ren, X.; Kong, Z.; Yang, J. & Zhang, S. The AmphiHex: A novel amphibious robot with transformable leg-flipper composite propulsion mechanism. *In* IEEE/RSJ International Conference on Intelligent Robots and Systems, Vilamoura-Algarve, Portugal, 2012, 3667–3672. doi: 10.1109/IROS.2012.6386238.
3. Wang, W.; Yu, J.; Ding, R. & Tan, M. Bio-inspired design and realization of a novel multimode amphibious robot. *In* IEEE International Conference on Automation and Logistics, Shenyang, China, 2009, 140–145. doi: 10.1109/ICAL.2009.5262958.
4. Ren, K. & Yu, J. Research status of bionic amphibious robots: a review. *Ocean Eng.* 2021, **227**, 108862. doi: 10.1016/j.oceaneng.2021.108862.
5. Ijspeert, A.J.; Crespi, A. & Cabelguen, J.M. Simulation and robotics studies of salamander locomotion. Applying neurobiological principles to the control of locomotion in robots. *Neuroinformatics*, 2005, **3**(3), 171-196. doi: 10.1385/NI:3:3:171
6. Farley, C.T. & Ko, T.C. Mechanics of locomotion in lizards. *J. Exp. Biol.* 1997, **200**(16), 2177–2188. doi: 10.1242/jeb.200.16.2177
7. Tang, Y.; Zhang, G.; Ge, D.; Ren, C. & Ma, S. Undulatory gait planning method of multi-legged robot with passive-spine. *Biomim. Intell. Robot.*, 2022, **2**(1), 100028. doi: 10.1016/j.birob.2021.100028
8. Rafeeq, M.; Toha, S.F.; Ahmad, S. & Razib, M.A. Locomotion strategies for amphibious robots-a review. *IEEE Access*, 2021, **9**, 26323-26342. doi: 10.1109/ACCESS.2021.3057406.
9. Xing, H.; Liu, Y.; Guo, S.; Shi, L.; Hou, X.; Liu, W. & Zhao, Y. Multi-sensor fusion self-localization system of a miniature underwater robot in structured and GPS-Denied environments. *IEEE Sens. J.*, 2021, **21**(23), 27136-27146. doi: 10.1109/JSEN.2021.3120663
10. Miglino, O.; Lund, H.H. & Nolfi, S. Evolving mobile robots in simulated and real environments. *Artif. Life*, 1995, **2**(4), 417–434. doi: 10.1162/artl.1995.2.4.417
11. Calandra, R.; Seyfarth, A.; Peters, J. & Deisenroth, M.P. Bayesian optimisation for learning gaits under uncertainty. *Ann. Math. Artif. Intell.* 2016, **76**(1–2), 5-23.

doi: 10.1007/s10472-015-9463-9

12. Agrawal, K.; Jain, K.; Gupta, D.; Shrivastava, R.; Agnihotri, A. & Thakur, A. Bayesian optimisation based terrestrial gait tuning for a 12-DOF alligator-inspired robot with active body undulation. *In* 42nd Mechanisms and Robotics Conference (MR), 2018, Quebec City, Canada.
doi: 10.1115/DETC2018-86033.
13. Spröwitz, A.; Tuleu, A.; Vespignani, M.; Ajallooeian, M.; Badri, E. & Ijspeert, A.J. Towards dynamic trot gait locomotion: Design, control, and experiments with cheetah-cub, a compliant quadruped robot. *Int. J. Rob. Res.,* 2013, **32**(8), 932-950.
doi: 10.1177/0278364913489205
14. Raibert, M.; Blankespoor, K.; Nelson, G. & Playter, R. Bigdog, the rough-terrain quadruped robot. *IFAC Proc.* 2008, **41**(2), 10822–10825.
doi: 10.3182/20080706-5-KR-1001.01833
15. Rebula, J.R.; Neuhaus, P.D.; Bonnlander, B.V.; Johnson, M.J. & Pratt, J.E. A controller for the littledog quadruped walking on rough terrain. *In* IEEE International Conference on Robotics and Automation*,* Rome, Italy, 2007, 1467-1473.
doi: 10.1109/ROBOT.2007.363191
16. Park, H.W.; Park, S. & Kim, S. Variable-speed quadrupedal bounding using impulse planning: Untethered high-speed 3D Running of MIT Cheetah 2. *In* IEEE International Conference on Robotics and Automation*,* Seattle, WA, USA, 2015, 5163-5170.
doi: 10.1109/ICRA.2015.7139918
17. Crespi, A.; Karakasiliotis, K.; Guignard, A. & Ijspeert, A.J. Salamandra robotica II: An amphibious robot to study salamander-like swimming and walking gaits. *IEEE Trans. Robot.* 2013, **29**(2), 308-320.
doi: 10.1109/TRO.2012.2234311
18. Zhong, B.; Zhou, Y.; Li, X.; Xu, M. & Zhang, S. Locomotion performance of the amphibious robot on various terrains and underwater with flexible flipper legs. *J. Bionic Eng.*, 2016, **13**(4), 525-536.
doi: 10.1016/S1672-6529(16)60325-6
19. Karwa, K.G., Mondal, S., Kumar, A. & Thakur, A. An open source low-cost alligator-inspired robotic research platform. Proceedings: 6th International Symposium on Embedded Computing and System Design*,* 2016, Patna, India.
doi: 10.1109/ISED.2016.7977088
20. Jia, X.; Frenger, M.; Chen, Z.; Hamel, W.R. & Zhang, M. An alligator inspired modular robot. *In* IEEE International Conference on Robotics and Automation*,* Seattle, WA, USA, 2015, 1949-1954.
doi: 10.1109/ICRA.2015.7139453
21. Hof, A.L.; Gazendam, M.G.J. & Sinke, W.E. The condition for dynamic stability. *J. Biomech.*, 2005, **38**(1), 1-8.
doi: 10.1016/j.jbiomech.2004.03.025
22. McGeer, T. Passive dynamic walking. *I.J. Robot. Res.*, 1990, **9**(2), 62-82.
doi: 10.1177/027836499000900206
23. Komatsu, H.; Ogata, M.; Hodoshima, R.; Endo, G. & Hirose, S. Development of quadruped walking robot Titan-XII and basic consideration about mechanics of large obstacle climbing. *In* The 2nd IFToMM ASIAN Conference on Mechanism and Machine Science. Tokyo, Japan, 2012, oai:t2r2.star.titech.ac.jp:50189082
24. Hutter, M.; Gehring, C.; Jud, D.; Lauber, A.; Bellicoso, C.D.; Tsounis, V.; Hwangbo, J.; Bodie, K.; Fankhauser, P.; Bloesch, M.; Diethelm, R.; Bachmann, S.; Melzer, A. & Hoepflinger, M. ANYmal - a highly mobile and dynamic quadrupedal robot. *In* IEEE/RSJ International Conference on Intelligent Robots and Systems, Daejeon, Korea (South), 2016, 38-44.
doi: 10.1109/IROS.2016.7758092
25. Buehler, M.; Battaglia, R.; Cocosco, A.; Hawker, G.; Sarkis, J. & Yamazaki, K. SCOUT: A simple quadruped that walks, climbs, and runs. *In* IEEE International Conference on Robotics and Automation*,* Leuven, Belgium 1998. 1707-1712.
doi: 10.1109/ROBOT.1998.677408
26. Kurazume, R.; Byong-won, A.; Ohta, K. & Hasegawa, T. Experimental study on energy efficiency for quadruped walking vehicles. *In* IEEE/RSJ International Conference on Intelligent Robots and Systems, Las Vegas, NV, USA, 2003, 613-618.
doi: 10.1109/IROS.2003.1250697
27. Kurazume, R., Yoneda, K. & Hirose, S. Feedforward and feedback dynamic trot gait control for quadruped walking vehicle. *Autonomous Robots*, 2002*,* **12**, 157-172.
doi: 10.1023/A:1014045326702
28. Gehring, C.; Coros, S.; Hutter, M.; Bloesch, M.; Hoepflinger, M.A. & Siegwart, R. Control of dynamic gaits for a quadrupedal robot. *In* IEEE International Conference on Robotics and Automation, Karlsruhe, Germany, 2013, 3287-3292.
doi: 10.1109/ICRA.2013.6631035
29. Maleki, S.; Parsa, A. & Ahmadabadi, M.N. Modeling, control and gait design of a quadruped robot with active spine towards energy efficiency. *In* International Conference on Robotics and Mechatronics*,* Tehran, Iran, 2015, 271–276.
doi: 10.1109/ICRoM.2015.7367796
30. Horvat, T.; Karakasiliotis, K.; Melo, K.; Fleury, L.; Thandiackal, R. & Ijspeert, A.J. Inverse kinematics and reflex based controller for body-limb coordination of a salamander-like robot walking on uneven terrain. *In* International Conference on Intelligent Robots and System*,* Hamburg, Germany, 2015 195-201.
doi: 10.1109/IROS.2015.7353374
31. Li, M.; Jiang, Z.; Wang, P.; Sun, L. & Ge, S.S. Control of a quadruped robot with bionic springy legs in trotting gait. *J. Bionic Eng.* 2014, **11**(2), 188-198.
doi: 10.1016/S1672-6529(14)60043-3
32. Willey, J.S.; Biknevicius, A.R.; Reilly, S.M. & Earls, K.D. The tale of the tail: limb function and locomotor mechanics in alligator mississippiensis. *J. Exp. Biol.* 2004, **207**(3), 553–563.
doi: 10.1242/jeb.00774
33. Fish, F.E.; Frappell, P.B.; Baudinette, R.V. & MacFarlane,

P.M. Energetics of terrestrial locomotion of the platypus ornithorhynchus anatinus. *J. Exp. Biol.*, 2001, **204**(4), 797–803. doi: 10.1242/jeb.204.4.797

34. Blob, R.W. & Biewener. Mechanics of limb bone loading during terrestrial locomotion in the Green Iguana (Iguana Iguana) and American Alligator (Alligator Mississippiensis). *J. Exp. Biol.* 2001, **204**(6), 1099-1122. doi: 10.1242/jeb.204.6.1099
35. Parrish, J.M. The origin of crocodilian locomotion. *Paleobiology*, 1987, **13**(4), 396-414. doi: 10.1017/S0094837300009003
36. Raj, A., & Thakur, A. Fish-inspired robots: Design, sensing, actuation, and autonomy: A review of research. *Bioinspiration and Biomimetics*. 2016, **11**(3), 031001. doi: 10.1088/1748-3190/11/3/031001
37. Crespi, A. & Ijspeert, A.J. Online optimisation of swimming and crawling in an amphibious snake robot. *IEEE Trans. Robot.* 2008, **24**(1), 75-87, doi: 10.1109/TRO.2008.915426
38. Saggar, M.; D'Silva, T.; Kohl, N. & Stone, P. Autonomous learning of stable quadruped locomotion, Rob. 2006 Robot Soccer World Cup X, (RoboCup 2006), Berlin, Heidelberg, 2006, **4434**, 98-109. doi: 10.1007/978-3-540-74024-7_9
39. Erden, M.S. & Leblebicioğlu, K. Free gait generation with reinforcement learning for a six-legged robot. *Rob. Auton. Syst.*, 2008, **56**(3), 199-212. doi: 10.1016/j.robot.2007.08.001
40. Li, Z.; Cheng, X.; Peng, X.B.; Abbeel, P.; Levine, S.; Berseth, G. & Sreenath, K. Reinforcement learning for robust parameterized locomotion control of bipedal robots. *In* IEEE International Conference on Robotics and Automation, Xi'an, China, 2021, 2811–2817. doi: 10.1109/ICRA48506.2021.9560769
41. Rofer, T. Evolutionary gait-optimisation using a fitness function based on proprioception, Rob. 2004 Robot Soccer World Cup VIII (2004), **3276**, 310-322. doi: 10.1007/978-3-540-32256-6_25
42. Chernova, S. & Veloso, M. An evolutionary approach to gait learning for four-legged robots. *In* IEEE/RSJ International Conference on Intelligent Robots and Systems*,* Sendai, Japan, 2004, 2562-2567. doi: 10.1109/IROS.2004.1389794
43. Weingarten, J.D.; Lopes, G.A.D.; Buehler, M.; Groff, R.E. & Koditschek, D.E. Automated gait adaptation for legged robots. *In* IEEE International Conference on Robotics and Automation, New Orleans, LA, USA, 2004, 2153-2158. doi: 10.1109/ROBOT.2004.1307381
44. Kohl, N. & Stone, P. Policy gradient reinforcement learning for fast quadrupedal locomotion. *In* IEEE International Conference on Robotics and Automation*,* New Orleans, LA, USA*, 2004,* 2619-2624. doi: 10.1109/ROBOT.2004.1307456
45. Santos, C.P. & Matos, V. Gait transition and modulation in a quadruped robot: A brainstem-like modulation approach. *Rob. Auton. Syst.*, 2011, **59**(9), 620-634. doi: 10.1016/j.robot.2011.05.003
46. Koco, E. Locomotion control for electrically powered quadruped robot dynarobin. *Proceedings of the 19th International Conference on CLAWAR: Advances in Cooperative Robotics,* London, UK, 2016, 63-70.
47. Gehring, C.; Coros, S.; Hutler, M.; Bellicoso, C.D.; Heijnen, H.; Diethelm, R.; Bloesch, M.; Fankhauser, P.; Hwangbo, J.; Hoepflinger, M. & Siegwart, R. Practice makes perfect: An optimisation-based approach to controlling agile motions for a quadruped robot. I*EEE Robot. Autom. Mag.*, 2016, **23**(1), 34-43. doi: 10.1109/MRA.2015.2505910
48. Digumarti, K.M.; Gehring, C.; Coros, S.; Hwangbo, J. & Siegwart, R. Concurrent optimisation of mechanical design and locomotion control of a legged robot. *Mobile Service Robotics*, *World Scientific*, 2014, 315–323. doi: 10.1142/9789814623353_0037
49. RunBin, C.; YangZhen, C.; WenQi, H.; Jiang, W. & HongXu, M. Trotting gait of a quadruped robot based on the time-pose control method. *Int. J. Adv. Robot*. Syst., 2013, **10**(2), 148. doi: 10.5772/50979
50. Rohmer, E.; Singh, S.P.N. & Freese, M., V-REP: A versatile and scalable robot simulation framework. *In* IEEE/RSJ International Conference on Intelligent Robots and Systems. Tokyo, Japan, 2013, 1321-1326. doi: 10.1109/IROS.2013.6696520
51. Fossen, T.I.; Breivik, M. & Skjetne, R. Line-of-sight path following of underactuated marine craft. *IFAC Proceedings Volumes*, 2003, **36**(21), 211-216. doi: 10.1016/S1474-6670(17)37809-6
52. Rasmussen, C.E. & Williams, C.K.I. Gaussian Process for Machine Learning, MIT press. 2006, Cambridge, MA, USA.
53. Tesch, M.; Schneider, J. & Choset, H. Using response surfaces and expected improvement to optimize snake robot gait parameters. *In* IEEE/RSJ International Conference on Intelligent Robots and Systems*,* 2011, San Francisco, CA, USA, 1069-1074. doi: 10.1109/IROS.2011.6095076

ACKNOWLEDGEMENT

This work was partially supported by the Science and Engineering Research Board (SERB), Department of Science and Technology, Government of India, through the IMPACTING RESEARCH INNOVATION AND TECHNOLOGY-2 (IMPRINT-2) Project under Grant IMP/2018/000523. The author would also like to thank Dhawal Gupta, Krishna Agrawal, and Kushagra Jain, who contributed to the physical experiments while they were undergraduate students at IIT Patna.

CONTRIBUTORS

Dr Atul Thakur obtained PhD degree in mechanical engineering from the University of Maryland, College Park and working as an Associate Professor in the Department of Mechanical Engineering at the Indian Institute of Technology Patna. His research interest is broadly in physics-aware planning for robots interacting with unregulated and, to some extent, adverse physical environments.